Asian Journal of Engineering and Applied Technology
ISSN: 2249-068X (Print) | 3049-1959 (Online)
Journal Homepage: https://ajeat.com/
DOI: https://doi.org/10.70112/ajeat-2026.15.1.4339

Research Article

Reliability Modelling of a High Integrity Pressure Protection System (HIPPS) Using the Multiple Beta-Factor Approach for Enhanced Safety in Oil and Gas

Remigius Obinna Okeke[1*] and Praise Igochi Onu[2]
[1*,2]Department of Electrical and Electronic Engineering, University of Port Harcourt, Rivers State, Nigeria

Article Information

Article History
Received: 30 January 2026
Revised: 27 February 2026
Accepted: 31 March 2026
Published online: 5 April 2026

Keywords
High Integrity Pressure Protection Systems (HIPPS)
Common-Cause Failures (CCFs)
Multiple Beta-Factor (MBF)
Fault Tree Analysis (FTA)
Probability of Demand (PFD)

Correspondence*
remigius.okeke@uniport.edu.ng

ORCID
Remigius Obinna Okeke
https://orcid.org/0009-0007-2533-8330
Praise Igochi Onu
https://orcid.org/0000-0002-7335-7807

Abstract

High Integrity Pressure Protection Systems (HIPPS) are essential for ensuring that oil and gas facilities comply with safety standards, making it crucial to use reliable estimation methods to determine their ability to handle high-pressure situations. Common-cause failures (CCFs) are often overstated in traditional reliability modelling methods, such as the single beta-factor (β) model, because they assume uniform dependency levels across subsystems. This work presents an improved modelling framework using the Multiple Beta-Factor (MBF) method combined with Fault Tree Analysis (FTA) for a more realistic representation of subsystem-specific CCF behaviour. Despite the expected drop in HIPPS reliability and the growth of PFD over time, the MBF model consistently produces lower PFD values than the traditional β-model. The improvement in PFD performance estimated by the MBF model is 20.5%, with a PFD of 0.62 at 100 hours, as opposed to 0.78 from the β-model. This MBF–FTA integration ensures a more balanced distribution of dependency parameters among sensors, actuators, and logic solvers. The model's accuracy is well established through validation with RMSE and MAE. The outcomes indicate that MBF modelling can be used to provide a more accurate and conservative reliability assessment for HIPPS.

I. INTRODUCTION

The high risk and complexity of process systems in the oil and gas sector make it fundamentally challenging to protect production assets from overpressure events. Overpressure can cause rupture, explosion, and catastrophic equipment failure; it also affects people, the environment, and the economy [1]. High Integrity Pressure Protection Systems (HIPPS) are designed to act as critical safety barriers and isolate the source of overpressure before it reaches downstream equipment. Safety Instrumented Systems (SIS) form the third layer of protection in industrial safety hierarchies, after inherent process design and alarm/interlock systems [2]. This grouping includes HIPPS. Three main subsystems make up a HIPPS: pressure transmitters, which sense an overpressure condition; a logic solver that reads sensor inputs; and final control elements (valves) that isolate the process section under abnormal conditions [3]. The use of redundancy architectures such as 1oo2, 2oo3, or 2oo4 voting logic is common in these systems to enhance reliability and minimize the occurrence of spurious shutdowns [4]. Even with this redundancy, HIPPS may face common-cause failures (CCFs) that occur simultaneously in multiple components because of shared influencing factors such as environmental stress, design flaws, or maintenance errors [5]. The probability of failure on demand (PFD) is an assessment factor for the reliability of HIPPS, indicating the system's increasing risk of failing to execute its required safety functions when needed [6]. As clearly stated in IEC 61508 and IEC 61511 standards, this is a significant factor in determining the system's Safety Integrity Level (SIL). Conventional reliability studies typically use the beta-factor (β) model to estimate the impact of CCFs. The model's assumption of a single dependency factor among components

oversimplifies real-world dependencies in redundant safety systems [7]. More recent studies have moved toward finer approaches, such as the MBF model. The MBF framework can capture multiple CCF pathways more appropriately by separating dependencies among different component groups [8]. MBF measures reliability through multiple correlated failure probabilities, which improves model sensitivity and predictive accuracy. When used with Fault Tree Analysis (FTA) for system-level reliability modelling, MBF provides both deductive logic mapping and probabilistic interdependency representation [6][9].

Research utilizing the Multiple Beta-Factor (MBF) approach in safety-instrumented systems has demonstrated significant advantages in approximating real reliability behaviour. Reference [10] showed that MBF can model redundant systems with interrelated failure paths more efficiently than conventional methods because it provides a more realistic representation of the complexity of CCF interactions. Despite this, there is a dearth of studies that explicitly apply the MBF model to HIPPS reliability, particularly in dynamic oil and gas operational settings where multiple subsystems interact under high stress. This study measures both independent and common-cause failures, determines the average PFD for general purposes, and compares its results with those of the traditional beta-factor model. It is anticipated that the outcomes will assist safety engineers in adopting more data-driven reliability modelling methods that support proactive system health monitoring and improved operational safety in oil and gas installations.

II. LITERATURE REVIEW

A. Overview of HIPPS Reliability Modelling

The High Integrity Pressure Protection Systems (HIPPS) are considered a crucial component of the third protection layer in the hierarchy of process safety barriers, designed to prevent equipment failure due to overpressure. Typically, HIPPS functions under the guidelines of IEC 61511 and IEC 61508, using sensors, logic solvers, and final control elements integrated to isolate hazardous pressure surges [11]. Unlike conventional pressure relief devices, HIPPS can independently shut down the process when certain thresholds are exceeded, resulting in a faster and more reliable response than mechanical relief valves [4]. HIPPS reliability is typically assessed using the probability of failure on demand (PFD), which indicates the likelihood that the system will fail when required [6]. In oil and gas systems, the determination of average PFD and SIL rating is crucial for system validation and certification because failures can be catastrophic [12].

B. Reliability Modelling and Common Cause Failures

Reliability modelling of HIPPS is challenged by Common-Cause Failures (CCFs), which arise from shared causes such as design errors, environmental stresses, or maintenance practices and may cause redundant components to fail simultaneously [5]. The probability of correlated failures has traditionally been represented using the Beta-Factor (β) model, which assumes a uniform dependency factor among components and may not accurately reflect the intricate interdependence of modern safety systems [6]. According to [7], the use of the beta-factor model can adversely affect HIPPS assessment by resulting in higher average PFD, lower availability, and increased accident frequency. Research has shifted toward more robust probabilistic methods, such as the Multiple Beta-Factor (MBF) model, because of these limitations [13].

By identifying various dependency paths and permitting variable correlations across component groups, the MBF model augments the traditional beta-factor approach. Using the MBF framework, [13] concluded that MBF can be used to analyse reliability parameters even with incomplete data. Similarly, MBF has been applied with Markov and time-domain analysis to evaluate the reliability of subsea control modules under different failure-detection rates. These studies highlight the versatility of MBF for modelling intricate fault relationships, particularly where data are scarce or uncertain.

C. HIPPS Safety Loop

In HIPPS, each safety loop controls the pressure values delivered by the three pressure transmitters. The three values are measured individually by limit monitors, each set to issue a signal as long as the measured value remains below the preset threshold. The HIPPS limit monitors are set within the elements presented in Fig. 1. The system design includes dedicated logic functions for pressure-transmitter maintenance, HIPPS reset operations, and routine Emergency Shutdown Valve (ESDV) testing. HIPPS architectures in the process industries are typically built around redundancy and voting logic to ensure high safety integrity while maintaining operational availability. As noted in [14], a common arrangement involves the use of three independent pressure transmitters that function as limit monitors within an out-of-three (2oo3) voting scheme. The voting output can continue to function under this arrangement as long as two transmitters indicate pressure values below a predetermined safety threshold. Typically, when one transmitter goes beyond this level, it is treated as a diagnostic alarm and sent to the ICSS rather than immediately initiating shutdown. This is intended to preserve fault tolerance and reduce spurious trips [15].

The use of the same safety-instrumented functions within a solid-state logic solver is standard for high-integrity protection systems. The underlying design of logic solvers, as described in [12], is intended to ensure safe failure behaviour, redundancy, and deterministic execution. By implementing redundant interlocking and blocking functions on open signals, the control logic in this framework facilitates maintenance on individual pressure transmitters. Whenever an operator applies a maintenance override, the voting logic removes the output of the selected limit monitor. This results in a controlled degradation of the voting architecture from 2oo3 to one-out-of-two (1oo2), as described in functional-

safety design guidelines [16], which allows maintenance activities without the complete suppression of the protection function. If any abnormal pressure is detected by one of the active transmitters, it will cause a HIPPS shutdown, thereby continuing to reduce risk during maintenance.

The allocation of logic solver modules that directly correspond to the analog acquisition modules is a recommended approach for improving fault tolerance in modular safety systems. A set of pressure transmitters is linked to each logic module, which means that any failure or removal of a single logic module will affect only one upstream and one downstream transmitter. Under these circumstances, the HIPPS continues to operate rather than falling into a degraded 1oo2 configuration, which is an approach aligned with availability-focused safety design principles discussed in both [16] and the wider HIPPS literature [15]. Modular redundancy enables the system to operate in fault-critical situations and maintains the required Safety Integrity Level (SIL) without degradation.

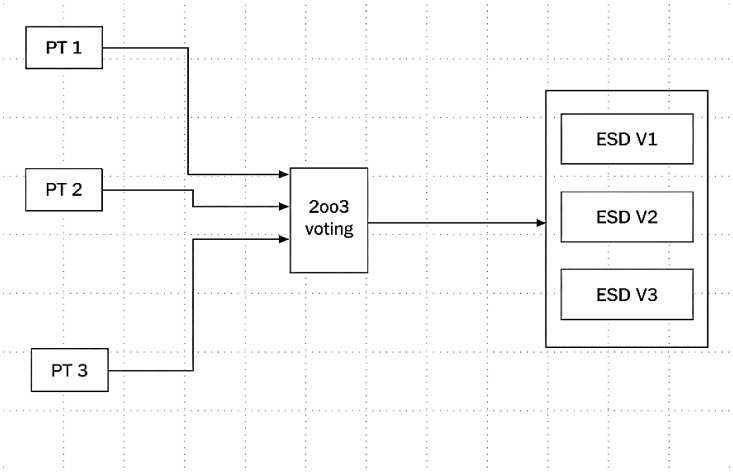

Fig.1 High Integrity Pressure Protection Systems (HIPPS) Safety Loop

D. Integration of Fault Tree Analysis (FTA) and Multiple Beta-Factor (MBF) Models

In recent reliability studies, Fault Tree Analysis (FTA) and MBF modelling have become increasingly interwoven. Boolean logic gates enable the logical breakdown of system failures into root causes through FTA, while MBF introduces a probabilistic correction for correlated failure [6]. This hybridization is beneficial for both diagnostic clarity and predictive power. According to [5], MBF within FTA can enhance understanding of inter-subsystem dynamics, while CCF sensitivities vary depending on the system configuration, including serial, parallel, and bridge connections.

Building on these foundations, [11] introduced the Dynamic Bayesian Network (DBN) model to simulate time-based reliability degradation under various testing regimes. That study identified a gap in measuring average PFD and in adequately testing system integrity under CCF influence. FTA and beta-factor models are often inadequate because they oversimplify the probabilistic variation among subsystems, particularly in HIPPS. Markov and Bayesian methods are useful, but they often do not account for the k-out-of-n voting logic that is a key feature of HIPPS sensor architecture (2oo3). Although not captured in many models, combined failure dependencies can also arise from the correlation of CCF propagation between logic solvers and actuators.

The use of MBF-based FTA provides a more compact and precise model for reliability analysis, as it integrates HIPPS reliability metrics with SIL compliance standards. The integration of MBF into FTA represents a gradual shift towards data-driven, simulation-based reliability modelling for high-risk industrial systems.

III. METHODOLOGY

A. Materials

In this section, we consider the quantitative analysis of a high-integrity pressure protection system in order to determine its functional and failure behaviour and evaluate its reliability. This quantitative model helps to determine the common-cause failure (CCF) probability in systems where redundancy is used to improve reliability, such as HIPPS. This research utilizes various materials and components, which are:

Logic Controller
Pressure Valve Controller
MATLAB/Simulink
Personal Computer
Pressure Sensor

B. Method

The method used in this research is the Multiple Beta-Factor (MBF) approach. The Multiple Beta-Factor model is a

reliability model that helps quantify the common-cause failure (CCF) probability in systems where redundancy is used to improve reliability, such as HIPPS. Again, the Multiple Beta-Factor is an advanced reliability-analysis approach that uses multiple beta factors to account for different common failures in redundant systems, thereby providing a more accurate estimate of system reliability. The method is used to account for common failures in redundant systems. It assumes that a certain fraction of failures in redundant components is attributable to a beta factor.

C. *Multiple Beta-Factor (MBF) Model*

The MBF model is a reliability and statistical method used to analyse and calculate the reliability and PFD for HIPPS. It accounts for multiple failure paths and their interaction.
MBF does the following:

The calculations identify the potential failure paths and their probabilities.It calculates the beta factor (BF) for each failure paths Calculates the PFD for each failure path. It combines beta factors using the MBF formula.

$$MBF = 1 - \pi(1 - \beta_i) \quad (1)$$

Where β_i is the beta factor for each failure path.
The MBF model gives a clear understanding of the probability of failure and the reliability of HIPPS. It better accounts for complex system interaction, provides more accurate failure-probability estimates, and optimizes system design and maintenance for HIPPS.

The closer the MBF value is to 0, the lower the PFD. When the MBF value is greater than 0, the PFD is higher. An MBF-derived PFD of 0.0249 is more acceptable than a PFD of 1. The common-cause failure values of HIPPS components at different failure paths and their beta factors are shown below.

Sensor 1 fails at 0.02
Sensor 2 fails at 0.02
Sensor 3 fails at 0.02
Logic solver 1 fails at 0.01
Logic solver 2 fails at 0.01
MBF = 1 - (1-0.02)3 X (1 – 0.01)2
MBF = 0.07754

D. *Modelling of HIPPS using Fault Tree Analysis (FTA)*

1. Basic Event Probability:

$$P_i = 1 - e^{-\lambda_i t} \quad (2)$$

The FTA is classified as one the top-down deductive method used in reliability analysis to systematically identify and assess the causes of system failures, focusing on how component failures contribute to the failure of the overall system. It is effective for High Integrity Pressure Protection Systems (HIPPS) because it models complex interactions between subsystems (e.g., sensors, logic solvers, valves) and helps quantify failure probabilities, ensuring safety and compliance in critical applications.

In a HIPPS, the FTA might show that the top event (system failure) results from either sensor malfunction, logic solver errors, or valve actuation failure, breaking down these failures using logic gates like OR and AND. This equation calculates the failure probability of a basic event i over time t using the distribution exponent, such that λ_i is the rate of failure of the event, where:
P_i is the failure probability of a basic event i
λ_i is the failure rate of the basic event i per unit time
t is the time period during which failure is considered.

2. Gate Probability for AND Gate:

$$P_{AND} = \prod_{i-1}^{n} P_i \quad (3)$$

This equation calculates the probability of failure for an AND gate in the fault tree, where all inputs must fail for the gate to fail.
P_{AND}: Probability of failure for the AND gate
P_i is the failure probability of each input basic event to the AND gate
n is the number of input events to the AND gate

3. Gate Probability for OR Gate:

$$P_{OR} = \prod_{i-1}^{n} (1 - P_i) \quad (4)$$

This equation calculates the probability of failure for an OR gate for the fault tree, where the gate fails if at least one input fails.
P_{OR} is the failure probability for the OR gate
P_i is the failure probability of each input basic event to the OR gate
n is the number of input events to the OR gate

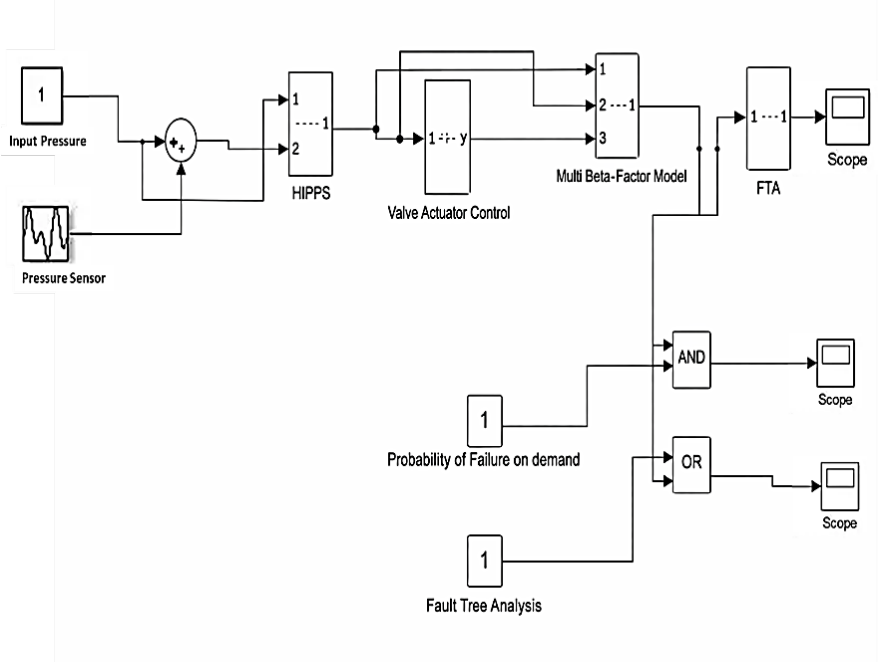

Fig.2 Simulink Diagram of the Multi Beta Factor Model System

4. Minimal Cut Sets Calculation:

$$P_{cut} = \sum_{j=1}^{m} P_{AND_j} \quad (5)$$

This equation sums the probabilities of failure for all the minimal cut sets present in the fault tree, where each cut set represents a unique combination of failures leading to the top event, where:
P_{cut} is the failure probability of the minimal cut set
P_{AND_j} is the failure probability of each of the minimal cut set AND gate.
m is the number of minimal cut sets.

5. Top Event Probability:

$$P_{TOP} = P_{OR} \quad (6)$$

This equation is for the top-level OR gates, and similarly for AND gates and it determines the probability of the top event failure in the fault tree, depending on whether the gate at the top level is an OR or AND gate, where:
P_{TOP} is the top event failure's probability.

E. Evaluation of the Realized Failure Rate Sequence on Common Cause Failures (CCF) with Multiple Beta-Factor (MBF) Model

1. Failure Rate of CCF with MBF: The failure rate with the Multiple Beta-Factor model is used to assess the likelihood that failures in multiple components arise because of a shared cause, thereby affecting equipment reliability. This model accounts for the correlation between components, recognizing that certain failures may not be independent but rather influenced by a common underlying factor. The failure rate is calculated by applying a set of beta factors, which quantify the strength of the dependency between the components in the system. By incorporating the MBF model, the system's failure behaviour can be more accurately predicted, especially when multiple components are vulnerable to similar failure modes. This methodology facilitates a more thorough understanding of aggregate risk, thereby contributing to the design of more robust systems through the consideration of both individual and common-cause failures.

$$\lambda_{CCF} = \lambda.\beta \quad (7)$$

This equation calculates the failure rate for a CCF using the MBF model, which adjusts the base failure rate by a beta-factor, where:
λ_{CCF}: Failure rate of the CCF
λ: Base failure rate of the components
β: Beta-factor representing the effect of common cause failures

2. Adjusted Failure Rate for n Components: The adjusted failure rate for (n) components considers the combined failure behaviour of multiple interconnected components within a system. It is derived by considering both the individual failure rates of each component and the effect of common-cause failures that may impact more than one component simultaneously. The adjusted failure rate incorporates the dependencies between components, which are modelled using techniques such as MBF. By modifying the failure-rate calculation, this approach yields a more precise depiction of the system's overall reliability by incorporating potential correlations among component failures. This adjusted failure rate is essential for designing more resilient systems and for evaluating the influence of CCFs on system safety and operational performance.

$$\lambda_{adj} = \lambda.\left(\frac{1-e^{-n\beta}}{n}\right) \quad (8)$$

This equation adjusts the base failure rate to account for the number of components n and their interaction through the beta-factor, where:
λ_{adj}: Adjusted failure rate considering multiple components
n: Number of components
β: Beta-factor

3. Probability of CCF: This likelihood that so many devices in a system fail due to a shared underlying cause. This probability is influenced by factors such as environmental conditions, design flaws, or systemic issues that affect several components simultaneously. Understanding the probability of CCF is critical to know the entire performance and protective hard equipment where interdependencies between components exist. By evaluating this probability, engineers can identify potential risks and implement mitigation strategies to reduce the likelihood of simultaneous failures in the system.

$$P_{CCF} = 1 - (1 - \lambda_{CCF})^n \quad (9)$$

This equation calculates the CCF probability affecting n components, considering their combined failure rate, where:
P_{CCF}: Probability of CCF
λ_{CCF}: Failure rate of CCF
n: Number of components

4. Effective Failure Rate: Including both individual components that failed and the consequences of common cause failures, the effective probability of failure in a system. The failure rates of individual components are compared to the likelihood that multiple factors contribute to simultaneous failures, which enhances the depiction of system reliability. If a component fails, the overall risk may be increased due to the correlations between components, leading to additional failure. The rate is then adjusted accordingly. Engineers can use the effective failure rate to determine the actual risk of system failures and then plan for redundancy and mitigation. The effectiveness of this calculation is crucial in maintaining the system's functionality and enhancing safety in hazardous situations.

$$\lambda_{eff} = \lambda.\left(1 + \frac{n-1}{\beta}\right) \quad (10)$$

This equation calculates the effective failure rate, incorporating the impact of multiple beta-factors on the base failure rate, where:
λ_{eff}: Effective failure rate
n: Number of components
β: Beta-factor

5. Failure Distribution for MBF: The (MBF) model employs the failure distribution to determine the likelihood of failures among various components in a system, considering their interdependence. The modeling of failure timing and probability is advantageous, as it allows for the simultaneous failure of various components due to shared causes. The MBF model uses beta factors to quantify the strength of these dependencies, allowing for a more accurate representation of the failure process compared to independent failure models. By incorporating the failure distribution, engineers can better understand the behaviour of the system over time and anticipate potential risks from correlated failures.

6. Realization of Failure Rate Sequence on Common Cause Failure (CCF) with the Multiple Beta-Factor (MBF): This section is about the realization of the failure-rate sequence on common-cause failure (CCF) with respect to the Multiple Beta-Factor (MBF). Equations have been designed or developed to describe the failure distribution over time for each parameter in terms of the Multiple Beta-Factor. Equation (11) describes this relationship.

$$f(t) = \lambda_{CCF}.e^{-\lambda_{CCF}t} \quad (11)$$

This equation describes the failure distribution over time for a component considering the MBF model.
$f(t)$: Failure distribution function over time
λ_{CCF}: Failure rate of CCF
t: Time

F. Compare the Influence of MBF with the Beta-Factor Model

The Multiple Beta-Factor (MBF) model improves on the traditional beta-factor model by accounting for dependencies among failures of different components rather than assuming that all components share the same common-failure dependency. This leads to more accurate predictions in systems with diverse failure sources, as the MBF model isolates correlated failures more effectively. The MBF model provides more accurate data when there are varying failure modes across components because it can account for partial common-cause failures, reducing the overestimation of risks typical of the traditional model.

1. Compare the Influence of MBF with the Beta-Factor Model: The influence of the Multiple Beta-Factor with respect to the beta-factor model is described in formulation (12), where the difference in failure rates between the MBF and beta-factor models is determined. The aim is to compare the MBF model with the traditional beta-factor model.

2. Comparison of Failure Rates:

$$\Delta_\lambda = \lambda_{MBF} - \lambda_{Beta} \quad (12)$$

This equation calculates the difference in failure rates between the MBF and beta-factor models, where:
Δ_λ: Difference in failure rates
λ_{MBF}: Failure rate with MBF model
λ_{Beta}: Failure rate with beta-factor model

3. Relative Improvement:

$$Relative\ Improvement = \frac{\lambda_{Beta}-\lambda_{MBF}}{\lambda_{Beta}} \quad (13)$$

This equation measures the relative improvement in failure rates when using the MBF model compared to the beta-factor model, where:
$Relative\ Improvement$: Improvement Ratio
λ_{Beta}: Failure rate with beta-factor model
λ_{MBF}: Failure rate with MBF model

4. PFD Difference Between Models:

$$\Delta_{PFD} = PFD_{MBF} - PFD_{Beta} \quad (14)$$

This equation calculates the difference in PFD values between the MBF and beta-factor models, where:
Δ_{PFD}: Difference in PFD values
PFD_{MBF}: PFD using MBF model
PFD_{Beta}: PFD using beta-factor model

5. Failure Probability Ratio:

$$Failure\ Rate = \frac{PFD_{MBF}}{PFD_{Beta}} \quad (15)$$

This equation calculates the ratio of failure probabilities between the MBF and beta-factor model, where:
$Failure\ Rate$: Ratio of failure probabilities
PFD_{MBF}: Failure probability with MBF model
PFD_{Beta}: Failure probability with beta-factor model

6. Effectiveness Comparison:

$$Effectiveness = \frac{SIL_{MBF}}{SIL_{Beta}} \quad (16)$$

This equation compares the effectiveness of the MBF model to the beta-factor model in achieving different SIL levels, where:
$Effectiveness$: Effectiveness Ratio
SIL_{MBF}: SIL level with MBF model
SIL_{Beta}: SIL level with beta-factor model

G. *Assess Functional Performance and Test Model Conformity*

Functional performance is typically assessed using criteria such as response time, reliability metrics such as mean time between failures, and the failure rate itself, which provide information about system efficiency and robustness. To evaluate the precision of predictive models, statistical validation techniques such as RMSE and MAE are employed to compare model predictions with real-world data. Through these assessments, the model can be adjusted to reflect real performance more accurately, enabling it to predict future outcomes more reliably.

1. Functional Performance Index (FPI):

$$FPI = \frac{P_{actual}}{P_{expected}} \quad (17)$$

This equation measures the functional performance of the HIPPS by comparing the actual performance to the expected performance, where:
FPI: Functional Performance Index
P_{actual}: Actual performance level
$P_{expected}$: Expected performance level

2. Model Accuracy Validation:

$$Accuracy = \frac{N_{correct}}{N_{total}} \quad (18)$$

By dividing the correct number of predictions by the predictions total number, (3.18) can calculate the accuracy of the model, where:
$Accuracy$: Proportion of correct predictions
$N_{correct}$: Number of correct predictions
N_{total}: Total number of predictions

3. Mean Absolute Error (MAE):

$$MAE = \frac{1}{N}\sum_{i=1}^{N}|P_{model.i} - P_{actual.i}| \quad (19)$$

This equation calculates the MAE of the model's predictions compared to actual values, giving an average magnitude of errors, where:
MAE: Mean absolute error of the model predictions
$P_{model.i}$: Predicted value for the i-th observation
$P_{actual.i}$: Actual value for the i-th observation
N: Total number of observations

4. Root Mean Square Error (RMSE):

$$RMSE = \sqrt{\frac{1}{N}\sum_{i=1}^{N}(P_{model.i} - P_{actual.i})^2} \quad (20)$$

This equation calculates the root mean square error of the model's predictions, providing a measure of the average magnitude of the prediction errors, where:
$RMSE$: Root mean square error of the model predictions
$P_{model.i}$: Predicted value for the i-th observation
$P_{actual.i}$: Actual value for the i-th observation
N: Total number of observations

5. System Performance Index:

$$SPI = \frac{P_{required}}{P_{observed}} \quad (21)$$

This equation assesses system performance by comparing the required performance level to the observed performance.
SPI: System Performance Index
$P_{required}$: Required performance level
$P_{observed}$: Observed performance level

6. Probability of Detection (PoD):

$$PoD = \frac{N_{detected}}{N_{actual}} \quad (22)$$

This equation measures the probability of detecting failures correctly by comparing the number of detected failures to the total number of actual failures.

PoD: Probability of detecting failures.
$N_{detected}$: Number of detected failures.
N_{actual}: Total number of actual failures.

7. False Alarm Rate (FAR):

$$FAR = \frac{N_{false\ alarm}}{N_{total\ trials}} \quad (23)$$

This equation calculates the rate of false alarms by dividing the number of false alarms by the total number of trials.
FAR: False alarm rate.
$N_{false\ alarm}$: Number of false alarms.
$N_{total\ trials}$: Total number of trials.

8. Coverage Probability:

$$Coverage = \frac{Number\ of\ Covered\ Failures}{Total\ NUmber\ of\ Failures} \quad (24)$$

This equation measures the proportion of failures covered by the system compared to the total number of failures.

9. Validation with Real-World Data:

$$Validation\ Score = \frac{\sum_{i=1}^{N} |P_{model.i} - P_{actual.i}|}{N} \quad (25)$$

This equation calculates the validation score by averaging the absolute differences between predicted and actual values, providing a measure of model accuracy.

TABLE I PARAMETERS OF THE RESEARCH

Parameter	Sign	Value	Unit	Description
Input Pressure	P_{in}	100	Bar	The pressure entering the system
Sensed Pressure	P_{sense}	98	Bar	Pressure detected by the sensor
Failure Rate	Λ	0.001	1/hr	The failure rate of a component
Proof Test Interval	T_{test}	8760	Hours	Time interval between proof tests
Probability of Failure on Demand	PFD	Cal. Value	-	Probability that the system will fail on demand
System Response Time	T_{resp}	1.5	Seconds	Time taken by the system to respond to input
Threshold Level	T_{level}	90	Bar	Pressure threshold for triggering HIPPS
Reliability	R	0.99	-	The reliability of the system
Beta Factor	β	0.1	-	Common cause failure factor

IV. RESULTS AND DISCUSSION

A. Reliability of the HIPPS Model

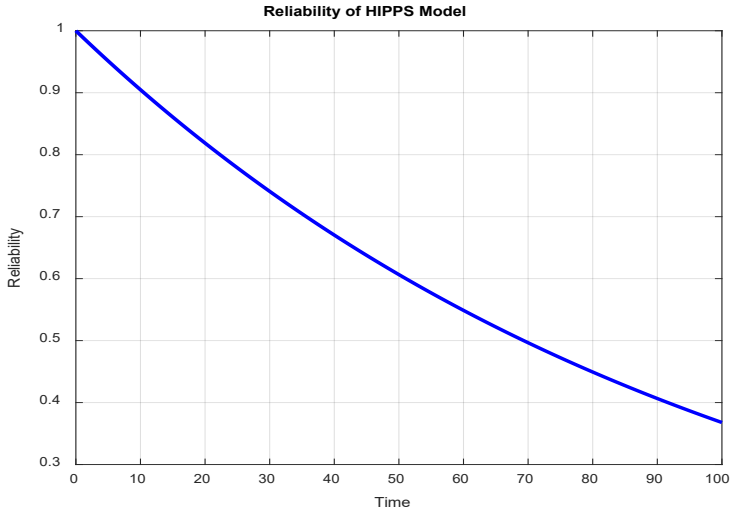

Fig.3 Reliability of HIPPS Model

In Figure 3, the graph illustrates the reliability of the HIPPS over time, with a notable point at which the reliability is shown to be 1 at 100 hours. This indicates that the system is completely secure, meaning that there is a 100% chance of the HIPPS meeting its protective function without failure during this period. A plot of HIPPS reliability using the MATLAB/Simulink environment is shown in the graph. The graph indicates that the HIPPS remains operational for a

significant amount of time, up to 100 hours, and can meet demand without degradation. This would mean it is operating under optimal conditions, where everything works as expected and external factors such as environmental stressors have not affected the reliability of the system at that point. Despite this, perfect reliability at 100 hours does not imply that the system will remain equally reliable over time during continued operation. The HIPPS must be monitored and maintained regularly to preserve reliability beyond 100 hours, particularly because of the impact of wear on various components.

B. Probability of Failure on Demand (PFD) vs. Time

In Figure 4, the graph depicting PFD versus time illustrates how the reliability of HIPPS changes over a 100-hour period. At the 100-hour mark, the figure from the MATLAB/Simulink simulation shows a PFD of 0.62, indicating that there is a 62% chance that the system will fail to perform its intended function when demanded at this specific time. The observed PFD level indicates a substantial decline in HIPPS reliability over time. This escalating PFD value signifies the accumulating effects of potential system failures, likely stemming from component degradation, environmental influences, or other operational factors that compromise system integrity. Consequently, as the system's operational lifespan extends, the probability of failure increases, thereby highlighting the necessity of consistent maintenance, vigilant monitoring, and potential system enhancements to uphold HIPPS reliability. The PFD of 0.62 at the 100-hour mark serves as a crucial indicator of compromised protective capability, which could present considerable hazards in industrial settings where HIPPS is essential for averting catastrophic failures, including overpressure events.

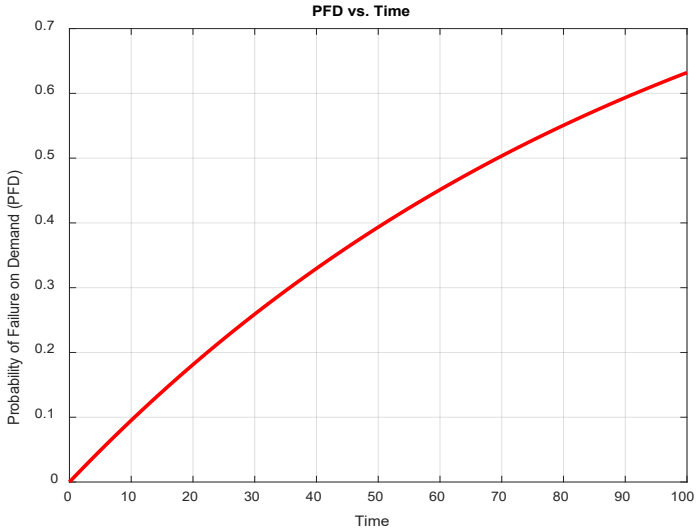

Fig.4 Probability of Failure on Demand (PFD) vs Time

C. Mbf Model and Beta Factor Model Comparison

In Figure 5, the graph presents a comparison between the PFD over time for a HIPPS using the MBF model and the traditional beta-factor model. The MBF model has a PFD of 0.62 at 100 hours, whereas the beta-factor model shows an equivalent value of 0.78. This contrast accentuates the different methods and assumptions used in these models, particularly in the way they deal with common-cause failures (CCFs) within the system. The MBF model's PFD of 0.62 at 100 hours indicates a more thorough understanding of CCFs because it acknowledges that different system components may have distinct vulnerabilities to these failures. The MBF model uses multiple beta factors to provide a more comprehensive assessment of system reliability, recognizing that failures in one component could cascade to others, particularly in complex industrial settings. This leads to the observed difference in PFD, suggesting a lower estimated likelihood of failure under the MBF model. Conversely, the beta-factor model's PFD of 0.78 at the same time assumes a uniform probability of failure across all components when considering common-cause failures. Although this simpler approach may be easier to apply, it can misrepresent the actual risk if the system has complex interdependencies. The lower degree of modelling fidelity may give a more optimistic or distorted view of reliability, possibly overlooking critical failure mechanisms that the MBF model captures. The difference in PFD values between these models at 100 hours underscores the importance of model selection in reliability evaluation. A lower PFD value in the MBF model indicates the value of more detailed analysis in high-risk environments, whereas the beta-factor model might be adequate in less complex situations. The selection of an appropriate model depends on the specific requirements of the HIPPS application and the degree of detail required for reliable predictions.

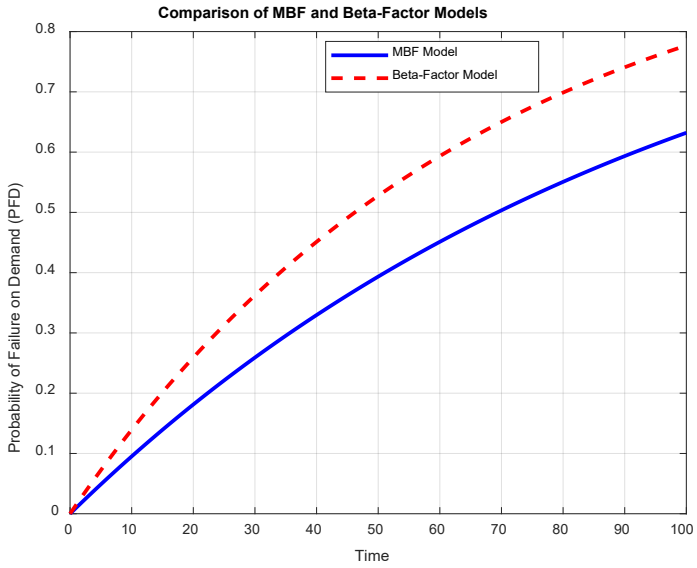

Fig.5 MBF and Beta Factor Comparison

D. Model Validation

The model-validation procedure is illustrated in Figure 6, where the MAE registers at 0.1% and the RMSE at 0.13%. These performance indicators are essential for evaluating the model's precision and dependability. The MAE of 0.1% signifies that, on average, the model's forecasts diverge from the actual data by only 0.1%. This minimal error margin underscores the model's high degree of accuracy, implying that the predictions closely align with the observed data and effectively represent the system's authentic dynamics. Although the RMSE of 0.13% is slightly higher, it remains very low, indicating that, while most predictions are precise, a small number exhibit marginally larger discrepancies. The marginal increase in RMSE compared with MAE suggests that the larger errors are negligible and do not substantially affect the model's overall efficacy. These metrics collectively validate the model's high degree of accuracy, demonstrating its capacity to closely mirror real-world scenarios with minimal error and establishing it as a dependable instrument for both system-performance analysis and prediction.

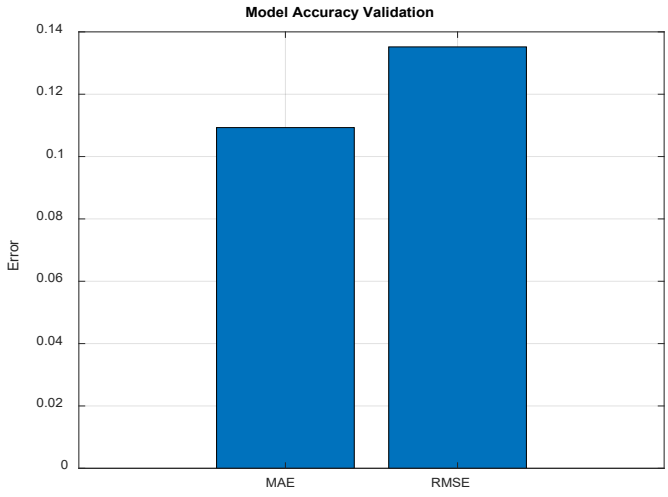

Fig.6 Model Accuracy Validation

E. The FTA for the HIPPS Analysis

Figure 7 illustrates the Fault Tree Analysis (FTA) outcomes for HIPPS, detailing the probabilities linked to various events and the top event. Within this analysis, the probabilities are defined as follows: (p1) = 0.01, (p2) = 0.02, and (p3) = 0.15. The probability of events occurring simultaneously for (p1) and (p2) is 0.001, while that of (p2) and (p3) is 0.00012, and the top event is predicted to occur at 0.00013. These values represent the probability of different failure scenarios in HIPPS. The individual events are unlikely to occur because the values for (p1) and (p2) are relatively low, indicating that these components are generally highly reliable. However, the higher value for (p3) may suggest that there is a greater

likelihood of this event occurring because of its nature or frequency. These events rarely occur simultaneously, as their combined probabilities are very low. The probability of the top event, although still small, indicates the likelihood of system failure when all contributing factors are taken into account. Despite the low individual probabilities and their combinations, the overall system reliability remains high, but careful management of the top event is still necessary.

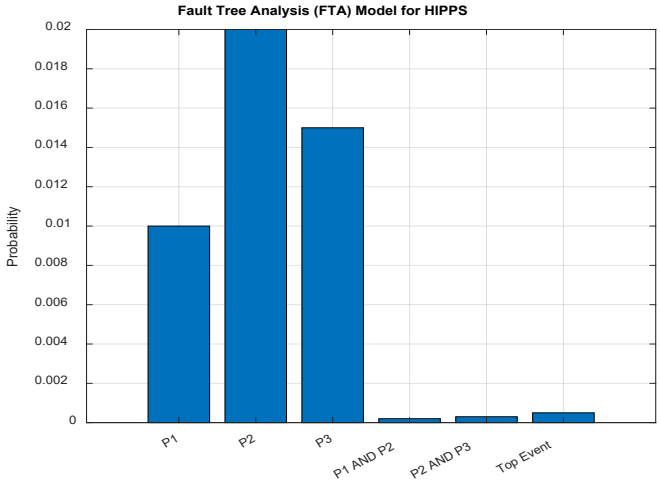

Fig.7 Fault Tree Analysis Model for HIPPS

F. Failure Rate Sequence on Common Cause Failures (CCF) for the Multiple Beta-Factor (MBF) Model

Figure 8 illustrates the failure-rate sequence for common-cause failures (CCF) using the MBF model for a system with 10 different failure events. The failure rates for these events are provided as follows: 0.01 for the first event, 0.008 for the second, 0.006 for the third, 0.0051 for the fourth, 0.0048 for the fifth, 0.0042 for the sixth, 0.00028 for the seventh, 0.0021 for the eighth, 0.0019 for the ninth, and 0.0015 for the tenth event. The observed sequence indicates a general decline in failure rates throughout the series of events. Initially, the failure rates are elevated, commencing at 0.01; however, they subsequently decrease, ultimately reaching 0.0015 by the tenth event. This downward trajectory implies that the probability of failures stemming from shared causal factors diminishes over time or across successive events. The elevated initial failure rates suggest a greater vulnerability to common-cause failures at the outset, possibly stemming from factors such as system configuration or the initial operational stages. Conversely, the reduced failure rates observed as the sequence advances imply enhanced reliability or more effective risk management, potentially resulting from system enhancements or the successful control of common-cause factors. Subsequently, this sequence offers perspectives on the temporal evolution of failure rates or their variation across distinct failure occurrences within the MBF model, thereby illuminating areas of heightened risk and the efficacy of risk-mitigation strategies deployed over time.

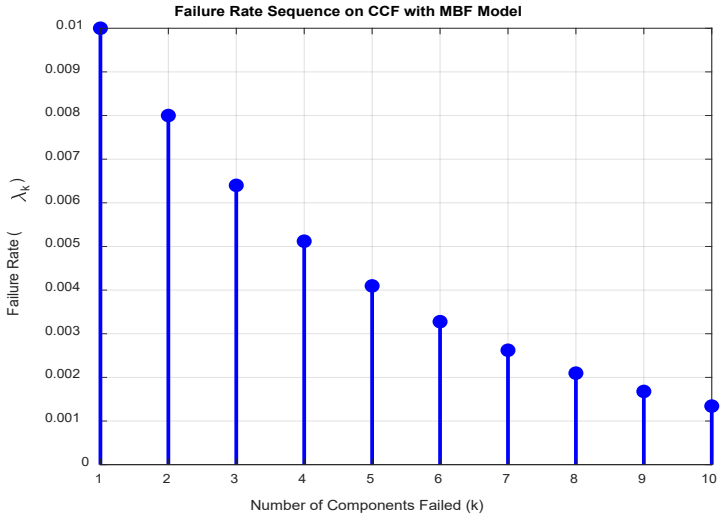

Fig.8 Failure Rate Sequence on CCF with MBF Model

G. Input Pressure

Figure 9 presents the input-pressure graph, which depicts the temporal evolution of pressure and is characterised by a distinct sinusoidal pattern that signifies periodic oscillations. Commencing from an initial baseline, the pressure exhibits a cyclical increase and decrease, thereby mirroring the system's inherent dynamism. This sinusoidal characteristic implies that the pressure experiences consistent perturbations, potentially stemming from operational parameters or environmental conditions.

The graph's regular oscillations reveal a consistent pattern, with the peaks and troughs representing the highest and lowest pressure levels recorded during the observation period. This fluctuation in input pressure is essential for understanding the system's response to dynamic conditions, especially in relation to HIPPS. By analysing these pressure variations, one can evaluate the system's capacity to maintain safety and reliability under diverse operational stresses, thereby confirming the effective functioning of HIPPS in preventing overpressure situations.

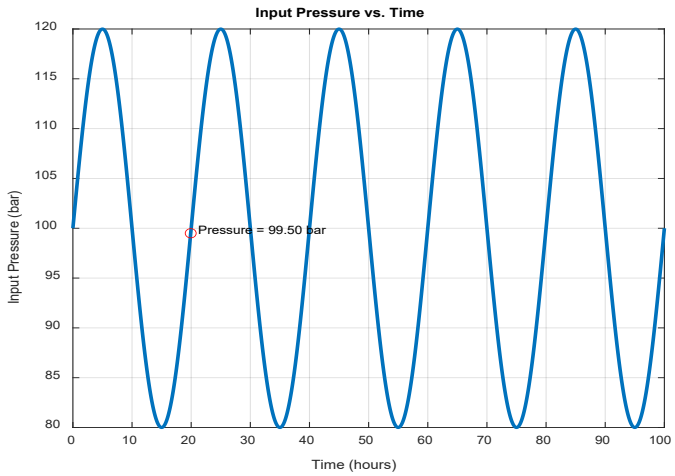

Fig.9 Input Pressure

V. CONCLUSION

This research developed a comprehensive reliability-modelling framework for HIPPS using the MBF model and Fault Tree Analysis (FTA). It was designed to better quantify the reliability performance of the system under various common-cause failure (CCF) dependencies and to compare model outputs with those of the traditional beta-factor approach. The results showed that HIPPS reliability naturally declines over time, while the probability of failure on demand (PFD) increases, indicating that periodic testing and maintenance are needed. Importantly, the MBF model produced lower PFD values than the beta-factor model at all simulation intervals. At 100 hours, the MBF model predicted a PFD of 0.62, while the beta-factor model predicted 0.78, representing a 20.5% difference. The improved performance of the MBF model can be attributed to its ability to depict subsystem dependencies rather than assume a uniform relationship among redundant components. The incorporation of MBF parameters into the FTA structure reduced their impact on the overall top-event probability and provided a more accurate picture of HIPPS reliability behaviour. Model validation using RMSE and MAE confirmed that MBF–FTA predictions align with anticipated reliability trends. These findings substantiate that the MBF–FTA modelling framework enhances reliability assessment by offering a more precise and critical interpretation of CCF effects. Consequently, the model supports better design decisions, efficient redundancy allocation, and improved SIL verification procedures for HIPPS and other safety-instrumented functions.

Declaration of Conflicting Interests
The authors declare no potential conflicts of interest with respect to the research, authorship, and/or publication of this article.

Funding
The authors received no financial support for the research, authorship, and/or publication of this article.

Use of Artificial Intelligence (AI)-Assisted Technology for Manuscript Preparation
The authors confirm that no AI-assisted technologies were used in the preparation or writing of the manuscript, and no images were altered using AI.

REFERENCES

[1] S. Mannan, "Lees' Loss Prevention in the Process Industries," Hazard Identification, Assessment and Control, Third Edition, 2012, https://doi.org/10.1016/B978-0-7506-7555-0.X5081-6.

[2] E. M. Marszal, and E. W. Scharpf, "Safety Integrity Level Selection: Systematic Methods Including Layer of Protection Analysis," International Society of Automation, 2009. ISBN: 978-1-945541-50-6.

[3] M. Rausand, and S. Haugen, "Risk Assessment: Theory, Methods, and Applications," John Wiley & Sons, 2020. ISBN: 9781119377238, https://books.google.com.ng/books?id=4yrPDwAAQBAJ.

[4] M. Cheraghi, and S. Taghipour, "Safety Integrity Level (SIL) evaluation of safety instrumented systems considering competing failure modes and subsystem priorities," Reliability Engineering & System Safety, vol. 260, 2025. ISSN 0951-8320, https://doi.org/10.1016/j.ress.2025.111025.

[5] S. B. Govardhan Rao, J. P. Castellanos-Ardila and S. Punnekkat, "A Systematic Review of β-factor Models in the Quantification of Common Cause Failures," 2023 49th Euromicro Conference on

Software Engineering and Advanced Applications (SEAA), Durres, Albania, pp. 262-269, 2023, https://doi.org/10.1109/SEAA60479.2023.00048.

[6] H. Jin, and M. Rausand, "Reliability of safety-instrumented systems subject to partial testing and common-cause failures," Reliability Engineering & System Safety, vol. 121, pp. 146-151, 2014, ISSN 0951-8320, https://doi.org/10.1016/j.ress.2013.08.006.

[7] S. Alizadeh, and S. Sriramula, "Reliability modelling of redundant safety systems without automatic diagnostics incorporating common cause failures and process demand," ISA Trans, pp. 599-614, https://doi.org/10.1016/j.isatra.2017.09.007.

[8] E. Zio, "Reliability engineering: Old problems and new challenges," Reliability Engineering & System Safety, vol. 94, no. 2, pp. 125-141, 2009, ISSN 0951-8320, https://doi.org/10.1016/j.ress.2008.06.002.

[9] M. Tanjin Amin, F. Khan, and S. Imtiaz, "Dynamic availability assessment of safety critical systems using a dynamic Bayesian network," Reliability Engineering & System Safety, vol. 178, pp. 108-117, 2018, ISSN 0951-8320, https://doi.org/10.1016/j.ress.2018.05.017.

[10] X. Wang, Q. Li and H. Zhou, "Modelling reliability of subsea control modules using MBF and Markov process," Ocean Engineering, no. 188, 106254, 2019.

[11] Y. Yu, Y. Liang, S. Wu, B. Cai, Y. Pan, R. Gao, S. Cheng, Y. Cui, Y. Yang, and H. Guo, "Safety performance evaluation of offshore high integrity pressure protection system using multiphase dynamic Bayesian network methodology," Ocean Engineering, vol. 310, no. 2, 2024, ISSN 0029-8018, https://doi.org/10.1016/j.oceaneng.2024.118620.

[12] IEC 61508, "Functional Safety of Electrical/Electronic/Programmable Electronic Safety-Related Systems," International Electrotechnical Commission, https://standards.globalspec.com/std/1250318/iec-61508-1.

[13] X. Wang, P. Jia, H. Lizhang, L. Wang, F. Yun and H. Wang, "Reliability and Safety Modelling of the Electrical Control System of the Subsea Control Module Based on Markov and Multiple Beta Factor Model," IEEE Access, vol. 7, pp. 6194-6208, 2019, https://doi.org/10.1109/ACCESS.2018.2889104.

[14] IEC 61511, "Functional Safety – Safety Instrumented Systems for the Process Industry Sector," International Electrotechnical Commission, https://26164953.s21i.faiusr.com/61/ABUIABA9GAAg5fmIjQYo1tntGA.pdf.

[15] A. E. Summers, "High Integrity Pressure Protection Systems (HIPPS): Design and Application." ISA Transactions, 2010. https://sis-tech.com/wpcontent/uploads/2015/10/High_Integrity_Pressure_Protection_Systems_Chapter.pdf.

[16] CCPS (Center for Chemical Process Safety), "Guidelines for Safe Automation of Chemical Processes," AIChE, 2019. https://www.everand.com/book/335956924/Guidelines-for-Safe-Automation-of-Chemical-Processes.